Concepts for lifetime efficient supply of power and heat to offshore installations in the North Sea

Luca Riboldi [a,*], Lars O. Nord [a]

[a]Department of Energy and Process Engineering, Norwegian University of Science and Technology - NTNU, Trondheim, Norway

Abstract

This paper assesses different concepts for efficient supply of power and heat to specific offshore installations in the North Sea, with the objective of cutting carbon dioxide emissions. The concepts analyzed include solutions with on-site power generation, full plant electrification, and hybrid solutions where power can be either generated locally or taken from the onshore grid. A detailed modeling of the power generation system was carried out, enabling design and off-design simulations. Plant power and heat demand profiles were used to evaluate the various concepts throughout the entire field's life. A first analysis of the common on-site power generation systems revealed the possibility of cutting carbon dioxide emissions simply by optimizing the operating strategy. Overall, the assessment of the different concepts showed that full plant electrification and the implementation of an offshore combined cycle have the potential to substantially reduce cumulative carbon dioxide emissions. A sensitivity analysis of the carbon dioxide emission factor, associated with the grid power, stressed how this parameter has a strong influence on the analysis outputs and, thus, needs to be thoroughly assessed. Similarly, the impact of increased plant heat demand was evaluated, showing that advantages connected to the plant electrification tend to diminish with the increase in heat requirements.

Keywords: offshore facilities; energy analysis; CO_2 emissions reductions; off-design simulations; electrification; combined cycle

Nomenclature

a	pressure drop acceleration loss term
A	heat transfer area, m^2
A_d	cross sectional flow area of the duct enclosing the bundle, m^2
A_n	net free area in a tube row, m^2
A_{nz}	the nozzle area at the steam turbine group inlet, m^2
C	dimensional constant
$C_{1\text{-}6}$	correction factors
C_f	friction factor
d_i	inner tube diameter, m
d_f	outside fins diameter, m
d_o	outside tube diameter, m

f	Fanning friction factor
G_n	mass velocity based on the net free area in a tube row, kg/s/m^2
h	convective heat transfer coefficient, W/m^2/K
H_f	fin height, W/m^2/K
HR_{plant}	plant heat rate, kJ/kWh
L	tube length, m
LHV_f	natural gas lower heating value, kJ/kg
$load_{GT}$	gas turbine load
$\dot{m}_f$	mass flow rate of natural gas used as fuel in the gas turbine, kg/s
$\dot{m}_s$	mass flow rate of steam in the steam turbine, kg/s
N_r	number of tube rows in the direction of flow
Nu	Nusselt number
p	pressure, Pa
p_{cond}	condenser pressure, bar
p_e	pressure at the steam turbine group outlet, Pa
p_i	pressure at the steam turbine group inlet, Pa
p_{steam}	steam evaporation pressure, bar
Pr	Prandtl number
R	steam turbine group pressure ratio correction factor (Stodola factor)
Re	Reynolds number
R_f''	fouling factor
R_{rad}	radiation resistance, K/W
R_{wall}	wall conduction resistance, K/W
T_f	fin temperature, K
T_g	gas temperature, K
T_{steam}	superheated steam temperature, °C
u	average flow velocity, m/s
U	overall heat transfer coefficient, W/m^2/K
v_i	specific volume at the steam turbine group inlet, m_3/kg
$\dot{W}_{aux}$	plant auxiliary power requirement, kW
$\dot{W}_{GT}$	gas turbine gross power output at generator terminals, kW
$\dot{W}_{GT,design}$	gas turbine gross power output at generator terminals at design conditions, kW
$\dot{W}_{net,plant}$	net plant power output, kW
$\dot{W}_{ST}$	steam turbine gross power output at generator terminals, kW
x_m	mean step quality

Greek letters

β	Baumann coefficient
Δp	gas-side pressure drop per pass, mbar
Δp_w	water-side pressure drop, mbar
ΔT_{cw}	condenser cooling water temperature difference, °C
ΔT_{OTSG}	pinch point temperature difference in the OTSG, °C
$\Delta\eta$	user-defined efficiency degradation
η_{dry}	dry step efficiency at design point
$\eta_{net,plant}$	net plant efficiency
η_{od}	dry step efficiency at off-design
η_{step}	corrected step efficiency

η_0	overall surface efficiency of a finned surface
ρ	fluid density, kg/m^3
ρ_b	average outside fluid density, kg/m^3
ρ_1	outside fluid inlet density, kg/m^3
ρ_2	outside fluid outlet density, kg/m^3
ϕ	flow function at off-design
ϕ_0	flow function at design
χ_{CO2}	CO_2 emission factor, kg/kWh

Acronyms

AC	alternating current
GA	genetic algorithm
GB	gas burner
GT	gas turbine
HR	heat rate
OTSG	once-through heat recovery steam generator
PFS	power from shore
SC	steam cycle
ST	steam turbine
WHRU	waste heat recovery unit

1. Introduction

The offshore processing of oil and gas is an energy-intensive sector, where natural gas is widely used to fuel equipment in the production, gathering and processing of gas and conventional crude oil. It has been estimated that petroleum extraction is the main contributor to greenhouse gas emissions in Norway, making up 28% of the total emissions in 2015 [1]. In 1991 Norway became one of the first countries in the world to introduce a CO_2 tax; this tax reached 1.02 NOK (0.12 $) per liter of petroleum or standard cubic meter of gas in 2016 [2]. In addition, Norway joined in 2008 the EU Emissions Trading System (EU ETS). It is becoming clear that improving the energy management of offshore installations opens up significant opportunities with regard to both cost savings and reduction of the environmental impact. In recent years, comprehensive thermodynamic analyses have been carried out on offshore facilities, pinpointing thermodynamic inefficiencies and estimating the potential for reducing energy and exergy losses. Some analyses were based on installations in the Norwegian Continental Shelf region. Different scenarios with respect to gas-to-oil and water-to-oil ratios were studied [3]. The variability of feed composition showed to have little influence on the breakdown of the thermodynamic irreversibilities. In order to assess potential differences in comparison to a field at the production peak, the situation on a mature field was analyzed in a following paper [4]. The operation on a real production day [5] was also investigated. The largest exergy destruction was noted in the processes involving pressure changes (compressors, pressure reduction valves and recycling), albeit the power generation unit was not taken into account. In another work, the same analysis framework was used to analyze and compare the oil and gas processing plants of four different North Sea offshore platforms [6]. Similar analyses were conducted for an offshore platform in the Brazilian Basin [7]. Despite the fact that the wide range of characteristics of offshore installations located in different areas (e.g. North Sea or Brazilian Basin) led to different conclusions, some common guidelines emerged. For instance, one of the main energy losses was the exhaust gases from simple gas turbines cycle. Several studies have investigated the feasibility of offshore combined cycles to exploit that energy, starting from the practical challenges related to the

installation of a bottoming cycle [8]. Kloster [9] argued for the technical and economic feasibility of offshore combined cycles using steam by reporting three successful offshore projects. The benefits of steam cycles (SCs) were further showed by Nord and Bolland [10], where process simulations showed a possible CO_2 emissions reduction of 20-25% in comparison to a simple gas turbine cycle. The possibility to use SCs for cogeneration of heat and power was also studied [11], resulting in potential cuts of CO_2 emissions between 9% and 22% depending on the heat requirements. Organic Rankine cycles (ORCs) were also thoroughly analyzed in the literature. The optimal design was studied by Pierobon et al. [12] through a multi-objective optimization process. Barrera et al. assessed the exergy performance [13] for offshore ORCs. Different ORC configurations were evaluated by Bhargava et al. [14], in connection with the gas turbines commonly used in offshore applications. A comparative analysis highlighted that SCs and ORCs are both attractive technologies for offshore applications [15]. The high working pressure typical of a CO_2 cycle leads to an increased compactness and makes these cycles interesting as well [16]. Another possible approach to improve energy efficiency involves electrification of the offshore facilities. Electrification has received strong political support recently. The Oil and Gas Department of the Norwegian Ministry of Petroleum and Energy instructs operators to look into the possibility of electrification of future offshore installations with power from shore. Electrification can be achieved with a connection to the onshore electric grid [17]. The integration of offshore wind power facilities with oil and gas installation and to the onshore grid was also proposed [18]. The grid integration did not show to be an issue, as the system demonstrated to withstand large disturbances [19]. Within certain conditions, offshore electrification has the potential to be beneficial both from a thermodynamic and environmental perspective, at the expense of high investment costs [20]. Projects involving the electrification of offshore installations have already been developed on the Norwegian continental shelf. The fields Ormen Lange, Snøhvit, Troll 1, Gjøa, Valhall and Goliat are supplied with power from shore [2]. An additional option is to integrate renewable energy sources to local power generation. Korpås et al. [21] discussed the possibility of operating an offshore wind farm in parallel with gas turbines, concluding that offshore wind is an economic and environmentally attractive option. Analyses could also be made by considering offshore areas as microgrids, to which apply advanced energy management systems for optimal operations [22].

The assessment of the various concepts for an efficient offshore energy supply has often been carried out in a single design point of the field life. Whilst the main equipment is normally designed to perform at peak conditions, power and heat requirements vary significantly over time. Therefore, for most of its life, the plant is operating at conditions far from design, with a consequent reduction of its efficiency. Accordingly, a correct evaluation of the real extent of CO_2 emissions reduction should take into consideration the different periods of a field's lifetime. There is a general shortage in the literature with regard to such a comprehensive approach. Nguyen et al. [23] presented a thermodynamic analysis of the life performance of an offshore platform by comparing three representative stages of an oil field (early-life, plateau and end-life production). Despite the energy requirements demonstrated to vary significantly over time, some findings were found to be valid for all production periods. In particular, the necessity of a better integration between the processing and power generation blocks of the plant was stressed. Advantages coming along with the introduction of a waste heat recovery cycles were also observed. Margarone et al. [24] analyzed the revamping options of an existing upstream gas facility by simulating one year of operation. By means of a flexible process simulation model, the following options were evaluated: (i) heat recovery from the incinerator exhaust gases, (ii) substitution of the low pressure (LP) – intermediate pressure (IP) turbine with an electric motor, and (iii) either a SC or an ORC using the gas turbines waste heat. The heat recovery from the incinerator and the substitution for the electric motors demonstrated to have a very short payback time. On the other hand, the addition of the ORC technology yielded a much better environmental performance. In another work, Mazzetti et al. [25] looked at an oil-

producing platform with a variable power-consumption profile over a 18-year period. The paper evaluated two scenarios: (i) the possibility to improve the performance of a simple gas turbine cycle by reducing the size of the gas turbines and, thus, operating at higher average relative load, and (ii) the addition of a CO_2 bottoming cycle. The first scenario achieved a 2% CO_2 emissions reduction. A 22% cut in CO_2 emissions could be achieved with the CO_2 bottoming cycle.

This paper aims to investigate and compare different concepts to supply power and heat to specific offshore plants in the North Sea. The case study, on which the analysis is based, is described in section 2. Several options have been proposed and deemed as feasible in the literature. The development of a common framework to allow fair and comprehensive comparisons between some of those concepts is a first contribution of this paper. The methods of analysis defined for this purpose are described in section 3, while the concepts assessed are outlined in section 4. For some of those concepts, an optimization of the operating strategy was carried out. The approach to the related optimization problems is presented in section 5. Section 6 reports the main results, with a sensitivity analysis on those parameters which were expected to significantly affect the results. Overall, the paper did not aim to provide an original contribution with regard to process modeling or metaheuristic optimization techniques. Those were the tools applied to pursue the paper's objective, which was to develop methods of analysis in order to assess the effectiveness of different concepts to supply energy to offshore installations. The contributions of the paper can be summarized as:

- Definition of a common framework for the comparative analysis of different concepts to supply power and heat to offshore installations.
- Detailed investigation of possible concepts and of their optimal operating strategy.
- Extension of the analysis to the entire lifetime of the plants rather than to specific conditions in order to evaluate the actual effectiveness of a concept.
- Application of the outlined analyses and methods to a case study.

2. Case study

The energy analysis implemented in the paper focuses on two specific offshore plants in the North Sea, namely Edvard Grieg and Ivar Aasen. The Edvard Grieg field has been developed with a production platform resting on the seabed, with a full process facility. The development of the Ivar Aasen field involved a production platform with a subsea installation tied to it. The first oil was delivered in late 2015 for Edvard Grieg and in late 2016 for Ivar Aasen. In both cases, a lifetime of approximately 20 years is expected.

The topside processing system of the plants under investigation consists of the following sections: production manifold, crude oil separation and stabilization, oil treatment, gas treatment, condensate treatment, fuel gas treatment, gas re-compression, oil pumping and water treatment. Heat and power are needed in order to operate such production facilities. In the first approximation, power is primarily needed for pumps (i.e. circulation of cooling water, water injection, oil export) and compressors (i.e. gas export, gas lift, gas re-injection), while a marginal fraction is supplied to other auxiliary functional units (i.e. Heating, Ventilation and Air Conditioning - HVAC, lights system). The main heat consumer is the oil separation process. This process involves the heating of the crude oil in order to reduce the viscosity and enhance crude/water separation. Another objective of the heating is the crude oil stabilization, which involves the boiling-off of the light hydrocarbons in order to provide stable crude for export. Crude oil separation and stabilization makes up for a large share of the heat requirement. Additional heat is required for other processing requirements (e.g. fuel gas heater) and utility demands.

A common development scheme was designed in order to meet the energy demand of both plants. The Edvard Grieg platform was equipped with two gas turbines (GTs) in order to generate and supply power to the plant. A dedicated alternating current (AC) cable connects the two platforms, allowing the GTs on Edvard Grieg to also cover Ivar Aasen's power demand. Oil and gas from Ivar Aasen are sent to the Edvard Grieg platform for further processing and export. Therefore, process heat requirements are located on Edvard Grieg, while Ivar Aasen's heat demand can be considered negligible. The current strategy is to provide process heat by exploiting the exhaust gases of the GTs. The extracted thermal energy is transferred to a heating medium in a separate heating circuit. The heating medium selected was pressurized water which further supplies heat to the processes.

The two offshore plants will be part of the electrification project involving the large Utsira High area. Starting from 2022, power will be taken from the local onshore grid in order to supply all the fields in the area [26]. The offshore platforms will be tied-in with AC cables and electrified. Given the electrification project, which is forecast to power the plants from 2022, the paper aims to investigate whether power from shore is actually the best option in terms of potential for CO_2 emissions reduction.

The offshore plants were simplified to two main blocks: the processing block and the power generation block, as shown in *Figure 1*. The processing block includes the process units taking care of the first treatment of the extracted hydrocarbons. The power generation block includes the equipment providing power and heat to the offshore plant. Depending on the specific operating conditions, the processing block has certain power and heat requirements. Such demand is met by the power generation block. Given this simplified representation, little information is needed to characterize the energy demand, namely: the magnitude of power and heat to supply to the processing block and the temperature at which the heat needs to be supplied. A more detailed breakdown of power and heat requirements was, thus, not investigated. The power and heat demand profiles throughout the lifetime of the offshore plants have been retrieved from the field development reports of Edvard Grieg [27] and Ivar Aasen [28], and are shown in *Figure 2*. The temperature of the process heat was provided by the operator of the plant and is reported in *Table 1*. At different heat demands the heating medium system was adjusted by varying the amount of water circulating, assuming that the same heat temperature is requested by the process units.

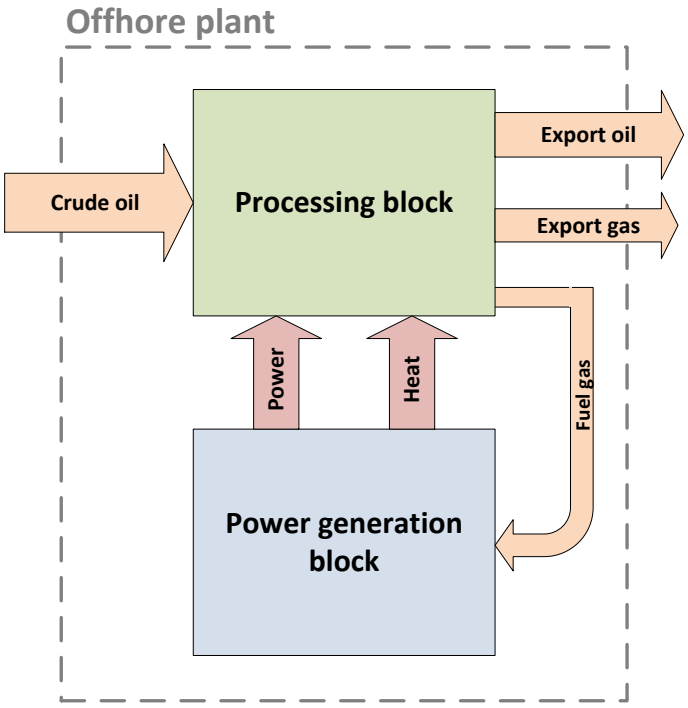

Figure 1. Simplified process scheme of the offshore plants.

While previous studies on the topic focused on a single design point, the current analysis considered several years of the plant's lifetime. Therefore, a profile of power and heat demand is provided rather than a single set of values. Such approach was used in order to have a more complete evaluation of the concepts. The time span considered begins with the year when power from shore (PFS) would be made available (2022) and includes all the production plateau years up to the depletion of the reservoir (2034). The power and heat demands were averaged on an annual basis, according to the information available. The plants' lifetime was, thus, described as an annual sequence of steady-state conditions. In accordance with that, the variations in energy requirements occurring at lower time spans (e.g. daily or hourly variations) were not considered and a dynamic model of the plant was not developed.

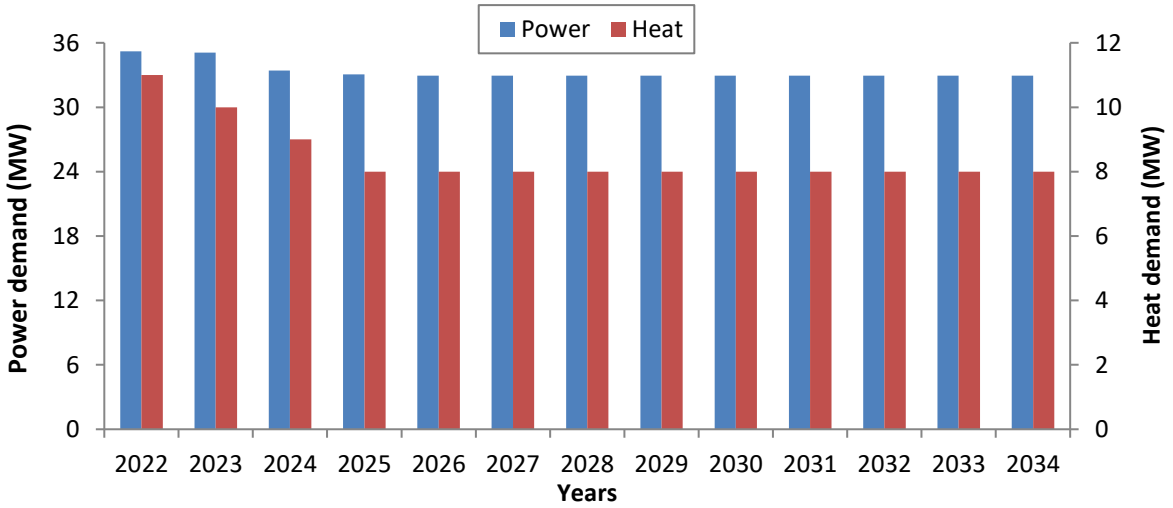

Figure 2. Power and heat demand throughout the years considered in the analysis.

In accordance with the scope of the paper, a thorough thermodynamic analysis of the processing block was not carried out. That kind of analysis can be useful to pinpoint inefficiencies in the plant design. This work, referring to a specific case study, considered the process plant design as given and intends to investigate solely the power generation block. Similarly, a plant retrofit aiming to improve the heat integration was not considered as it requires extensive knowledge of the processing block. Further, both theoretical (i.e. need for stable heat sources and consumers over time) and practical (i.e. space for new tubes and heaters) limitations would have arisen.

3. Methods

The flowchart shown in *Figure 3* gives an overview of the analysis framework developed to study the effectiveness of the different concepts investigated. The energy requirements of the specific case study were defined on an annual basis, as described in the previous section. Detailed process models of the power generation units were designed on the basis of those energy requirements, so to enable the simulation of the operation of the different concepts. Each concept was investigated in detail and its operating strategy was optimized seeking to maximize the energy efficiency and minimize the CO_2 emissions. A lifetime simulation was then carried out in order to provide a complete assessment of the concepts investigated. This approach focusing on the entire lifetime of the plants rather than on single occurrences aims to be a step forward for these kind of analyses. In line with that, the overall effectiveness of a concept was measured through cumulative performance indicators, specifically through the cumulative CO_2 emissions.

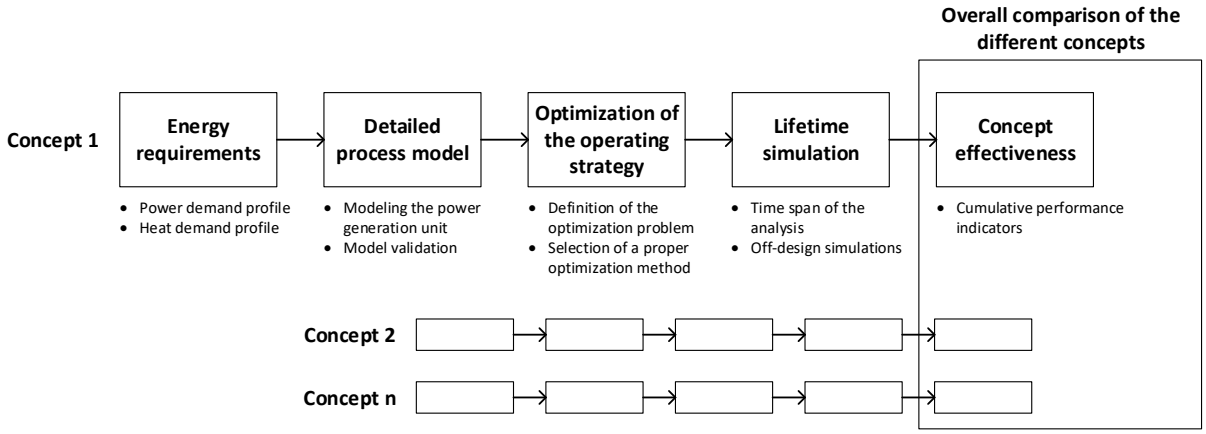

Figure 3. Flowchart of the different steps constituting the common framework for the comparative analysis between the various concepts investigated.

The remainder of this section includes descriptions of the performance indicators, of the modeling methods, and of the models' validation process.

3.1 Performance indicators

The main variables and performance indicators used in the analysis are outlined in this section.
The net plant efficiency was defined as:

$$\eta_{net,plant} = \frac{\dot{W}_{net,plant}}{\dot{m}_f LHV_f} \tag{1}$$

where $\dot{W}_{net,plant}$ is the net plant power output, $\dot{m}_f$ is the mass flow rate of natural gas used as fuel in the gas turbine, and LHV_f is the natural gas lower heating value.
The net plant power output was defined as:

$$\dot{W}_{net,plant} = \dot{W}_{GT} + \dot{W}_{ST} - \dot{W}_{AUX} \tag{2}$$

where $\dot{W}_{GT}$ is the gas turbine gross power output at generator terminals, $\dot{W}_{ST}$ is the steam turbine gross power output at generator terminals (this term applies when a steam bottoming cycle is present), and $\dot{W}_{AUX}$ is the plant auxiliary power requirement.
The plant heat rate was also defined as:

$$HR_{plant} = \frac{3600}{\eta_{net,plant}} \tag{3}$$

The GT load, which expresses the part-load operations of the GT, is defined as:

$$load_{GT} = \frac{\dot{W}_{GT}}{\dot{W}_{GT,design}} \tag{4}$$

where $\dot{W}_{GT,design}$ is the gas turbine gross power output at generator terminals at design conditions, i.e. GT operating at full load and at the specific site conditions (see *Table 1*). It is worth stressing the difference between the GT load, defined above, and the total plant load. The latter consists in the total power requirement of the offshore plant.

3.2 Carbon dioxide emission factor

A CO_2 emission factor (χ_{CO2}) was used to account for the CO_2 emissions connected to power from shore (PFS). Establishing which value to assign to this parameter throughout the years is a challenging task, though of paramount importance as it strongly affects the outputs. Once the boundaries of the analysis (e.g. the Nordic power system) are defined, this factor should consider the CO_2 emissions associated with the marginal increase in power production necessary to meet the offshore power demand. Since onshore power production is expected to undergo substantial changes in upcoming years, χ_{CO2} is also expected to vary significantly. The best approach would be to define a profile that returns a specific value of χ_{CO2} for each year. A complex model of the relative power system would need to be developed for the purpose, but that goes beyond the scope of the current paper. Therefore, the choice was to rely on a profile available in the literature (see *Figure 4*). In order to check the modeling assumptions and methodologies behind such a profile, reference should be made to [17]. The estimations were based on a prediction of the replacement power composition, i.e. the marginal power generated to cover the offshore demand. In early years the marginal power is made up mainly of coal power, while following natural gas power and renewable power are taking over a larger share. This explains the initial decreasing trend. Last years considered in the analysis are characterized by a growing share of lignite power, causing the emission factor to increase again. Given the uncertainty associated with this analysis, a

sensitivity analysis of the results will be presented, with χ_{CO2} set equal to the Nordic (0.10 kg_{CO2}/kWh [29]), Norwegian (0.02 kg_{CO2}/kWh [30]) and European (0.43 kg_{CO2}/kWh [29]) current values.

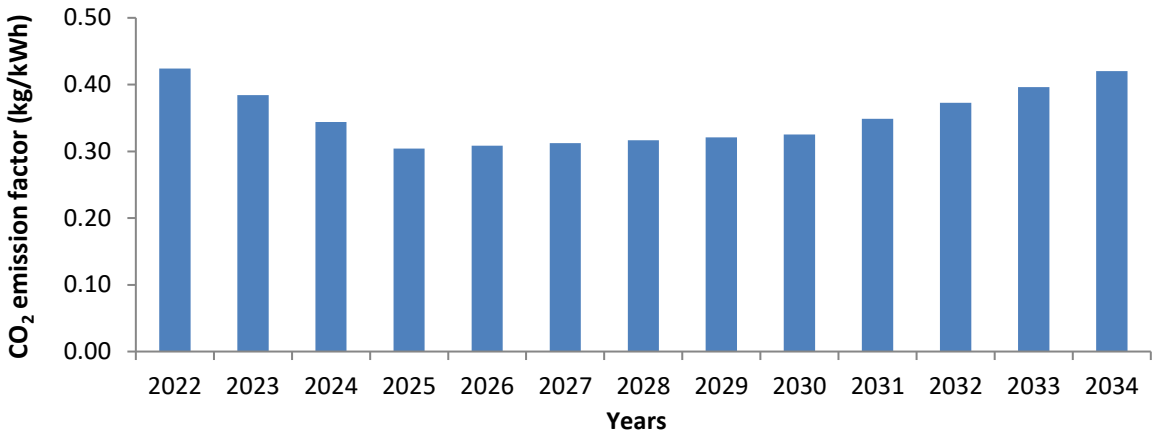

Figure 4. CO_2 emission factor associated with power from shore throughout the years considered in the analysis.

3.3 Modeling the power generation unit

THERMOFLEX (Thermoflow Inc.) [31] was the simulation platform used for the process modeling and simulation. THERMOFLEX is a fully-flexible program for design and off-design simulation of thermal systems. The modeling of the power generation unit consisted, in the base case, of the two GTs and a waste heat recovery unit (WHRU). The GT modeled was a GE LM2500+G4, selected from the Thermoflow library of gas turbine engines and was based on a data-defined model developed from vendor-supplied specifications. The WHRU was modelled as a counter-flow vertical finned tube heat exchanger. Pressurized water from the heating medium system circulated within the tubes and was heated by the exhaust gas stream flowing across the tubes. The physical hardware design was defined to reproduce the WHRU currently installed on the plant. A staggered tube layout with solid fins was applied. The geometry of the heat exchanger was specified in terms of fin sizes and spacing, and tubes sizes and spacing. Once the design was set, the inputs describing the hardware were used to compute the pressure drops on the gas-side and water-side, as well as the overall heat transfer coefficient, in accordance with the correlations in Eqs. (5)–(12).

Gas-side pressure drop [32]:

$$\Delta p = \left(f + a \right) \frac{G_n^2 N_r}{1.083 \cdot 10^9 \rho_b} \tag{5}$$

$$f = C_2 C_4 C_6 \left(\frac{d_f}{d_o} \right)^{0.5} \tag{6}$$

$$a = \frac{1 + \left(\frac{A_n}{A_d} \right)^2}{4 N_r} \rho_b \left(\frac{1}{\rho_2} - \frac{1}{\rho_1} \right) \tag{7}$$

where Δp is the pressure drop per pass, f is the Fanning friction factor, a is the pressure drop acceleration loss term, G_n is the mass velocity based on the net free area in a tube row, N_r is the number of tube rows in the direction of flow, ρ_b is the average outside fluid density, C_2-C_4-C_6 are correction factors, d_f is the outside fins diameter, d_o is the outside tube diameter, A_n is the net free area in a tube row, A_d is the cross

sectional flow area of the duct enclosing the bundle, ρ_2 is the outside fluid outlet density and ρ_1 is the outside fluid inlet density.

Water-side pressure drop:

$$\Delta p_w = \left(4C_f \frac{L}{d_i} + 2 \right) \frac{\rho u^2}{2} \tag{8}$$

$$C_f = \frac{0.046}{\mathrm{Re}^2} \tag{9}$$

where Δp_w is the water-side pressure drop, C_f is the friction factor, L is the tube length, d_i is the inner tube diameter, ρ is the fluid density, u is the average flow velocity and Re is the Reynolds number.

Overall heat transfer coefficient:

$$\frac{1}{UA} = \frac{1}{(\eta_0 hA)_w} + \frac{R''_{f,w}}{(\eta_0 A)_w} + R_{wall} + \frac{R''_{f,g}}{(\eta_0 A)_g} + \frac{1}{(\eta_0 hA)_g} + R_{rad} \tag{10}$$

where U is the overall heat transfer coefficient, A is the heat transfer area, η_0 is the overall surface efficiency of a finned surface, h is the convective heat transfer coefficient, R_f'' is the fouling factor, R_{wall} is the wall conduction resistance and R_{rad} is the radiation resistance. Subscripts w and g refer to water- and gas-side of the heat exchanger, respectively.

Gas-side convective heat transfer coefficient [32]:

$$Nu = C_1 C_3 C_5 \,\mathrm{Re}\,\mathrm{Pr}^{1/3} \left(\frac{T_g}{T_f} \right) \left(\frac{d_o + 2H_f}{d_o} \right)^{1/2} \tag{11}$$

where Nu is the Nusselt number, C_1-C_3-C_5 are correction factors, Re is the Reynolds number, Pr is the Prandtl number, T_g is the gas temperature, T_f is the fin temperature, d_o is the outer tube diameter and H_f is the fin height.

Water-side convective heat transfer coefficient:

$$Nu = 0.023\,\mathrm{Re}^{0.8}\,\mathrm{Pr}^{0.33} \tag{12}$$

The flue gas and water incoming thermodynamic states and mass flow rates were imposed by the network on the component, and the component determined the exit thermodynamic states. The thermal load is defined through the mass flow rate of water circulating in the heating medium system. In accordance with the plant specifications, a water loop was modeled where pressurized water (22 bar) enters the WHRU at 120°C and needs to be heated up to 170°C in order to meet the heat demand of the processing block. Tubing and pressure drops were defined in order to represent realistic offshore operating conditions.

One of the concepts studied included a steam bottoming cycle. The topping gas turbine cycle was based on a GE LM2500+G4 gas turbine. A once-through heat recovery steam generator (OTSG) was modeled to exploit the remaining thermal energy of the GT exhausts in order to raise superheated steam. Once-through heat recovery steam generator technology offers advantages in terms of compactness, weight limitations and flexibility which are of importance for offshore applications [10]. An OTSG can be described as a continuous heat exchanger in which the preheating, evaporation, and superheating of the

feedwater takes place. Unlike conventional heat recovery steam generators, there is no steam drum to separate the phases. The hardware design of each section of the OTSG has been carried out by selecting proper tube type, thickness, fin geometry and spacing. The basic characteristics were taken from the work by Nord et al. [33]. The temperature profile of the OTSG was based on Eqs. (5)–(12). The superheated steam leaving the OTSG was expanded in a steam turbine. The method to evaluate the steam turbine performance was based on the estimation of a constant dry step efficiency for each steam turbine's group. A semi-empirical efficiency estimation method, derived by [34], is first applied to define a group efficiency. The model iterated to find the value for the dry step efficiency for the group which will replicate the group efficiency. Each step was assumed to have the same pressure ratio as well as the same dry step efficiency. A correction was applied to all steps with steam quality below the Wilson line, according to:

$$\eta_{step} = \eta_{dry} - \beta\left(1 - x_m\right) \tag{13}$$

where η_{step} is the corrected step efficiency, η_{dry} is the dry step efficiency at the design point, x_{m} is the mean step quality and β is the Baumann coefficient.

Iterations were repeated until the computed group exit state matched that found from the semi-empirical method. The overall isentropic efficiency was finally calculated taking into account exhaust loss and valve throttling effect. The division into steps was convenient for off-design simulations, which utilized the design-point inlet flow function, adjusted nozzle area and dry step efficiency, for each group, to compute off-design pressures and efficiencies, as described in Eqs. (14)–(17).

$$A_{\mathrm{nz}} = \frac{C\,\dot{m}_s\sqrt{\frac{v_i}{p_i}}}{R} \tag{14}$$

$$R = \sqrt{1 - \left(\frac{p_e}{p_i}\right)^2} \tag{15}$$

$$\eta_{od} = \eta_{dry} - f\left(\frac{\phi}{\phi_0}\right) - \Delta\eta \tag{16}$$

$$\phi = \dot{m}_s\sqrt{\frac{u}{p}} \tag{17}$$

where A_{nz} is the nozzle area at the group inlet, C is a dimensional constant, $\dot{m}_s$ is the steam mass flow rate, v_{i} is the specific volume at the group inlet, p_{i} is the pressure at the group inlet, R is the group pressure ratio correction factor (Stodola factor), p_{e} is the pressure at the group outlet, η_{od} is the dry stage efficiency at off-design, f denotes a functional dependence which is determined according to [34], ϕ is the flow function at off-design, ϕ_0 is the design-point value of the flow function, $\Delta\eta$ is a user-defined efficiency degradation, u is the average flow velocity, p is the pressure.

A sliding pressure control mode was applied to the steam cycle. The inlet steam volumetric flow was kept close to constant resulting in very similar velocity vectors at different load points and, thus, in near-

constant isentropic efficiency for the steam turbine. For the off-design simulations, the steam temperature was controlled by the feedwater flow to the OTSG [35]. The heat rejection occurred in a deaerating condenser, modeled as a shell-and-tube heat exchanger, with sea water in the tube side. The design of the combined cycle, based on the work by Nord et al. [33], was then optimized in order to better match the specific operating conditions.

For the configurations with onshore power supply, the process heat demand was met with a gas-fired water heater. The heater was modelled to be able to meet peak heat demand and warm the water heating medium with an efficiency of 85%, in line with similar solutions in place on offshore installations. An air blower was included to feed air to the gas-fired heater. An isentropic efficiency of 80% was considered for the blower. The power from shore (PFS) was computed by taking into account a 99% transformer efficiency and a transmission loss term depending on the location of the power generation site (8% from Nordic region and 15% from central Europe). This term included losses on the HVDC cable connecting the platform to the shore and losses in the electrical grid transmission lines.

The fuel gas was natural gas, with a typical composition for an extracted gas in the North Sea. The site conditions were selected to average a year in the specific North Sea geographical location. *Table 1* sums up the assumptions used in the modeling.

Table 1. Site conditions and modeling assumptions

Site		**Natural gas**	
Ambient T (°C)	9.4	CH_4	72.9
Ambient P (bar)	1.013	C_2H_6	13.6
Frequency (Hz)	60	C_3H_8	8.3
Cooling water system	Direct sea water cooling	N_2	1.6
Cooling water T (°C)	10	CO_2	0.2
Gas Turbine		n-C_4H_{10}	1.8
GT fuel	Production gas	i-C_4H_{10}	0.9
LHV (MJ/kg)	47.4	n-C_5H_{12}	0.3
GT inlet ΔP (mbar)	10	i-C_5H_{12}	0.3
GT exhaust ΔP (mbar)	10	C_6H_{14} +	0.1
Waste heat recovery unit		**Once-through boiler**	
Tube material	T11	Tube material	Incoloy
Fin material	T409	Fin material	TP409
Fin type	Solid	Fin type	Serrated
Tube layout	Staggered	Tube layout	Staggered
Condenser		**Water loop**	
Condenser type	Dearating condenser	Inlet water T (°C)	120
Heat exchanger design	Shell-and-tube	Outlet water T (°C)	170
Electrification		**Gas-fired heater**	
Transmission losses	8–15 %	Efficiency	85%
Transformer efficiency	99 %	**Air blower**	
		Isentropic efficiency	80%

The lifetime simulation of the modeled power generation unit was obtained through a connection with MATLAB. Microsoft Excel was used as the interface between MATLAB and THERMOFLEX. MATLAB first provides inputs for each simulation (i.e. for each year) into Excel and subsequently calls for a simulation in THERMOFLEX. The connection between THERMOFLEX and Excel is ensured by the utility ELINK, which works with Thermoflow's core modeling software. The outputs of the simulation are then collected into the Excel sheet, conveyed to MATLAB and further processed.

3.4 Model validation

The performance map of the selected GT (i.e. GE LM 2500+G4) is based on a data-defined model developed by THERMOFLEX, built upon specifications and correction curves provided by the GT manufacturer. The obtained performance was, thus, deemed to be reliable. The model of the WHRU is based on and validated against industrial data. The performance of the combined cycle was validated against the paper from Nord et al. [33], which in turn was validated against the 2012 Gas Turbine World Handbook. A combined cycle with the same characteristics as those in the referenced paper was modeled in THERMOFLEX. *Table 2* shows the outputs for comparison. The differences in output values were lower than 1%.

Table 2. Performance comparison between an offshore combined cycle in the literature and one modelled in this work.

Combined cycle	Nord et al. [33]	This paper
Gas Turbine	GE LM 2500+G4	GE LM 2500+G4
Frequency (Hz)	60	60
NOx abatment	DLE	DLE
GT gross power (MW)	31.9	31.8
ST gross power (MW)	12.0	12.1
Net plant power output (MW)	43.5	43.5
Net plant efficiency	51.7 %	51.7 %
CO_2 emitted (kg/MWh)	387	385
Steam mass flow (kg/s)	11.0	11.1

4. Concepts for lifetime efficient supply of power and heat

The following concepts were evaluated:

- **GTs + WHRU**: local offshore power generation meets the plant's energy demand, with no power taken from onshore. The power is produced by two GTs (2 X GE LM2500+G4), while the heat is extracted from the relative exhaust gases by means of a WHRU. Different operating strategies were tested in order to allocate the total plant load between the two GTs at the different operating conditions. The first one (A) consists of equally splitting the power demand between the GTs. This is normally the strategy utilized in offshore installations for the sake of flexibility and responsiveness of the power generation unit, thus it is considered as the base case. The second operating strategy (B) consists of running one GT at maximum load, while the other is operated to provide the remaining power. The maximum load has been set at 90% in order to preserve a margin for maneuver in case a sudden load increase is necessary. If the load of the second GT drops to a value lower than the minimum allowed (i.e. arbitrary chosen to be 15%

when the GT has not to provide heat to the processes, otherwise 35%) then the strategy is to run this second GT at this lower limit, while the first GT is operated to match the plant power requirement. The final operating strategy (C) consists of allocating the load between the two GTs through an optimization process.

- **GT + WHRU + PFS**: this hybrid concept partially exploits the possibility of obtaining PFS, while simultaneously running a GT (1 X GE LM2500+G4) in order to meet the process heat requirement. The GT also provides an additional power contribution, which decreases the overall PFS needed. Three different operating strategies for splitting the power demand between the GT and the PFS are proposed. The first one (A) consists of running the GT at the minimum load able to provide enough heat to the processes. This minimum load has been conservatively estimated to be 35%, as at that operating condition the exhaust gases of the GT would be able to meet the heat demand of whichever year with a reasonable flexibility margin. PFS makes up the remaining power supply. The second operating strategy (B) consists of running the GT at maximum load (i.e. 90%) and, accordingly, at maximum efficiency. PFS makes up the remaining power supply. The third operating strategy (C) consists of running the GT at the maximum load or the minimum load able to provide heat, depending on the PFS CO_2 emission factor in the considered year. For instance, in years where the power produced onshore is credited with a high CO_2 emission factor, it may be more convenient to produce as much power as possible offshore, vice versa for years characterized by a low CO_2 emission factor. The objective is to minimize the CO_2 emissions irrespective of where those emissions occur.
- **GT + WHRU + SC**: the power demand is entirely covered through on-site production by using one GT (1 X GE LM2500+G4) and a steam bottoming cycle. Steam is raised in a OTSG and then expanded in a steam turbine. The process heat is supplied from the GT exhaust gases to the existing WHRU, while the downstream steam bottoming cycle exploits the remaining thermal power available in the gas. The design of the steam bottoming cycle was selected through a multi-objective optimization process. This case assumes that it is possible to install the necessary bottoming combined cycle equipment (i.e. OTSG, steam turbine, water condenser, etc.) on the platform. Footprint and weight issues may make this option questionable, although the removal of one GT from the platform could help with regard to that.
- **PFS + WHRU**: the power demand is entirely covered by PFS. A supplementary gas firing system is installed to provide heat by exploiting the existing WHRU. An air blower, providing combustion air, is included in the model, with the relative power consumption. The utilization of PFS entails a larger amount of export gas to be compressed and, consequently, increased power consumption. This power term has been obtained by modeling a gas compression process with an isentropic efficiency of 85%. The additional amount of gas to compress was evaluated by taking case GT + WHRU (A) as reference.
- **PFS + GB**: the power demand is entirely covered by PFS, and the platform is equipped with a gas burner. The gas-fired water heater ties-in to the existing heating medium system in order to provide process heat. An air blower, providing combustion air, is included in the model, with the relative power consumption. Similar to the previous case, the power to be supplied from onshore is increased by a term due to the larger amount of gas to compress.
- **PFS**: PFS covers the entire power and heat demand of the offshore plant. The heat is provided through electric heaters installed on the platforms. Similarly to the previous case, the power to be supplied from onshore is increased by a term due to the larger amount of gas to compress.

A total of 10 simulation cases were assessed:

1. GTs + WHRU (A)
2. GTs + WHRU (B)
3. GTs + WHRU (C)
4. GT + WHRU + PFS (A)
5. GT + WHRU + PFS (B)
6. GT + WHRU + PFS (C)
7. GT + WHRU + SC
8. PFS + WHRU
9. PFS + GB
10. PFS

Schematics of the cases described are represented in *Figure 5-10.*

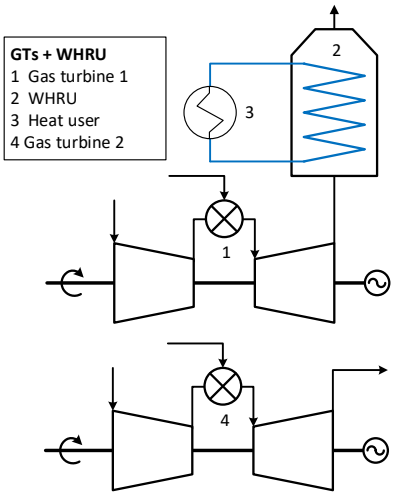

Figure 5. Schematic of the GTs + WHRU concept

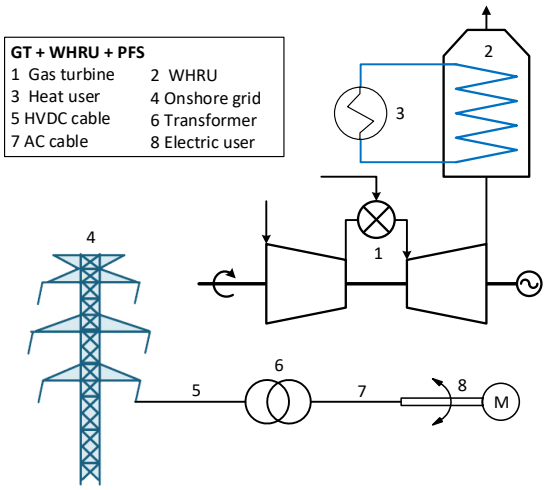

Figure 6. Schematic of the GT + WHRU + PFS concept

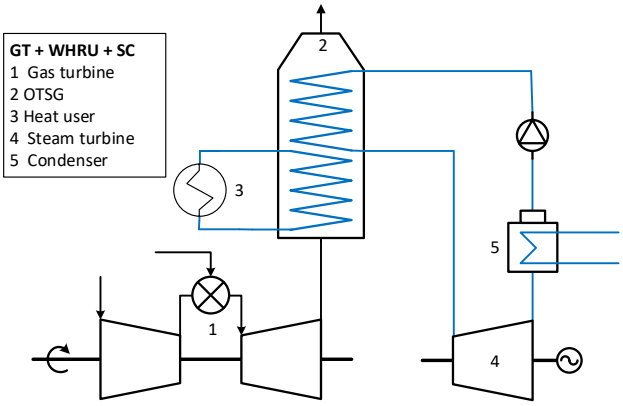

Figure 7. Schematic of the GT + WHRU + SC concept

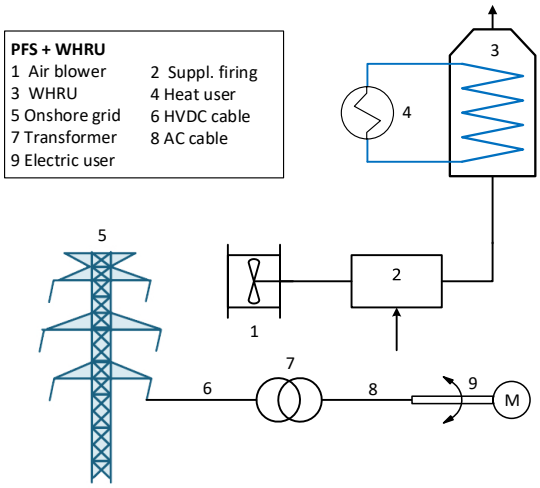

Figure 8. Schematic of the PFS + WHRU concept

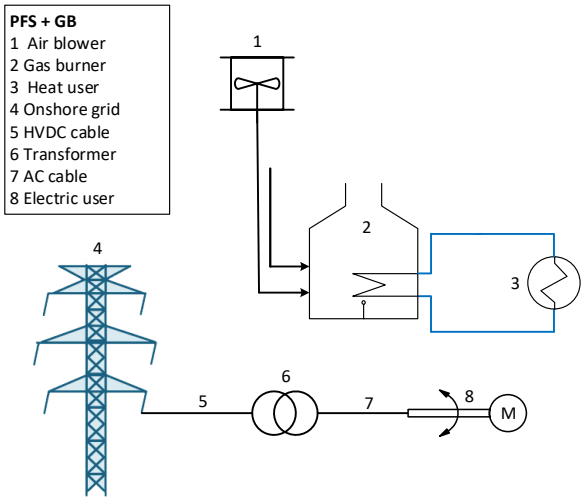

Figure 9. Schematic of the PFS + GB concept

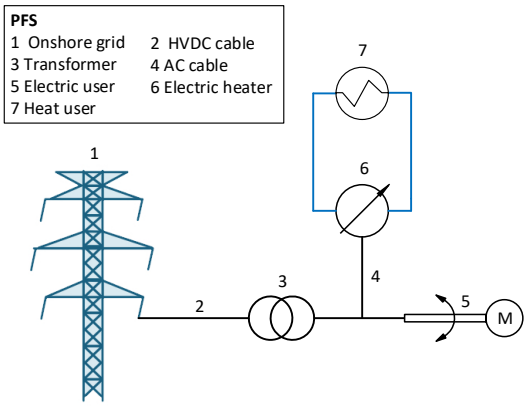

Figure 10. Schematic of the PFS concept

5. Optimization processes

The connection between the process simulation tool (i.e. THERMOFLEX) and MATLAB allows not only for a lifetime simulation of the offshore plants but also for additional optimization analyses. In this work two optimization problems were defined. The first one involved the optimization of the total plant load share between the two GTs. The second optimization process involved the definition of the optimal bottoming steam cycle design, according to the objective functions considered.

5.1 Optimal load allocation

The case termed GTs + WHRU (C) relied on an optimization process to define the optimal load allocation between the two GTs. The optimal configuration is that which produces the exact amount of power requested, while performing at maximum efficiency (thus with the minimum CO_2 emissions) and depends on the off-design performance map of the GTs. It is challenging to define a priori a strategy resulting in optimal performance for the different operating conditions. A similar optimization problem has been studied with regard to the load-allocation in a ship power plant and potential benefits have been pinpointed [36]. The optimization problem to be solved was of a black-box type as the simulation results are generated from THERMOFLEX, whose underlying model and solution strategy are not entirely known. In accordance with this consideration, derivative information could not be used for solving the optimization problem and a black-box optimizer needed to be selected. A review and benchmarking of such methods can be found in the literature. Rios and Sahinidis [37] reviewed those for unconstrained and bound-constrained problems. Martelli and Amaldi [38] focused on nonlinearly constrained problems. Among the options available, an elitist genetic algorithm (GA) was chosen. The GA, first introduced by Holland [39], is a method for solving both constrained and unconstrained optimization problems, which is based on natural selection, the process that drives biological evolution. The GA repeatedly modifies a population of individual solutions over a number of iterations called generations. At each step, the objective function – termed fitness function in this case – is evaluated and the “fittest” individuals (the parents) in a population have the best chance of surviving and passing on their genes to the next generation (the children). The new individuals are generated whether combining the vector entries of a pair of parents (crossover) or introducing random changes to individual parents (mutation). Some particularly fit individuals (elite) are also directly passed to the next generation. Over successive generations, the population "evolves" toward an optimal solution. The GA algorithm does not require

the objective function to be differentiable or continuous [37]. It was selected because it proved itself to be a reliable method for several process engineering problems [40]. It was also readily available within the MATLAB Global Optimization Toolbox [41]. If on one hand the GA guarantees robustness regarding numerical issues, such as numerical noise and discontinuities in the objective function, on the other hand it is a metaheuristic algorithm and, as such, it provides sub-optimal solutions. For the purposes of the analysis carried out in this paper, the approximation introduced was considered acceptable and more advanced algorithms were not investigated. Nonetheless, it is worth stressing that what is termed "optimum" throughout the paper could have been termed "the near global optimum." Despite that, the wording "optimum" was retained, for the sake of simplicity.

For the specific problem, the objective function was set as the minimum total heat rate of the power generation system, which is the inverse of the efficiency and is directly related to the CO_2 emissions. The decision variable considered was simply the load of one GT (the other load was determined accordingly in order to meet the power demand). The load of the GT was allowed to vary between 90% (maximum load) and 15% (minimum load). The crossover fraction was specified, which indicated the fraction of each population, other than elite children, that are made up of crossover children. An adaptive termination condition was selected as stopping criterion for the GA. The GA stopped when the average relative change in the fitness function value over a number of stall generations was less than the function tolerance. The GA parameters were specified as follows:

- Population size 25
- Number of stall generations 10
- Function tolerance 10^{-5}
- Crossover fraction 0.8

5.2 Optimal steam bottoming cycle design

Defining the proper design of an offshore steam bottoming cycle is a challenging task, which involves different and, possibly, conflicting requirements. For the relative simulation case (i.e. GT + WHRU + SC), a multi-objective optimization problem was set in order to identify the Pareto frontier of solutions with minimum heat rate (ergo the maximum net plant efficiency) and minimum weight. The effectiveness of using a Pareto approach to multi-objective optimization has been stressed in the literature [42]. It is well known that, in offshore applications, minimizing the weight is of paramount importance, as it is maximizing the efficiency. The total weight term used as objective function accounts for the augmented weight due to the introduction of additional equipment, including the once-through boiler, the steam turbine, the generator and the (wet) condenser. Evolutionary algorithms (like GA) are particularly suitable to tackle multi-objective optimization problems [43], as they deal simultaneously with a set of possible solutions (the so-called population) which allows finding several members of the Pareto-optimal set in a single run of the algorithm. Additionally, evolutionary algorithms are less susceptible to the shape or continuity of the Pareto frontier. The main challenge is to minimize the distance of the generated solutions to the Pareto set and to maximize the diversity of the developed Pareto set. The GA from the MATLAB Global Optimization Toolbox [41] was again used for the presented multi-objective optimization problems. GA-based methods have already been successfully applied to similar multi-objective optimization problems, for example for the design of a SC [33]. The optimization variables were defined as being among those having the largest influence on the bottoming cycle performance and weight. The selected variables were: (i) steam evaporation pressure p_{steam}, (ii) superheated steam temperature T_{steam}, (iii) pinch point temperature difference in the OTSG ΔT_{OTSG} (iv) condenser pressure p_{cond} and (v) condenser cooling water temperature difference ΔT_{cw}. These variables are listed in *Table 3*, together with the lower and upper bounds defined for the optimization problem.

Table 3. List of decision variables, with upper and lower bounds, used in the optimization process for the design of the steam bottoming cycle.

	Lower bound	Upper bound
Decision variables		
p_{steam} (bar)	15	35
T_{steam} (°C)	300	410
ΔT_{OTSG} (°C)	10	30
p_{cond} (bar)	0.03	0.12
ΔT_{cw} (°C)	3	10

The crossover fraction was again set equal to 0.8. The algorithm stopped when either the average change in the spread of Pareto solutions, a measure of the movement of the Pareto frontier, was less than the function tolerance over a number of stall generations or when the maximum number of generations was exceeded. The GA parameters were specified as follows:

- Population size 50
- Number of stall generations 5
- Function tolerance 10^{-3}
- Maximum number of generations 250
- Crossover fraction 0.8

6. Results and discussions

In this section the main results obtained are reported and discussed. Firstly, the optimization processes are taken into consideration. The optimal load allocation between the GTs and the optimal design of the bottoming steam cycle were determined. The outputs of these optimization processes paved the way for the following lifetime performance analysis of the concepts studied.

6.1 Plant load share optimization between the gas turbines

The load optimization problem determined the most efficient way to allocate the power demand between the two GTs in the base case of our analysis (GTs + WHRU). *Figure 11* shows the share of power generation between the first (GT1) and second (GT2) gas turbines for the three operating strategies considered, of which the case termed (C) relies on the optimized outputs. Equally splitting the power generation between the two GTs (case A) is often the preferred solution on the ground of flexibility. In the case of an unexpected trip of a gas turbine, the other can rapidly take over a large fraction of the missing load. However, the analysis of the optimum load allocation revealed that such an approach is the least efficient, at least for the power requirements tested. On the contrary, the second operating strategy (B) is often very close to the most efficient option. In fact, the optimized case (C) shows that optimal GT loads substantially match those of the second case (B) for most of the plant's lifetime. For a more detailed insight, *Table 5* in the Appendix reports all the GT loads selected in the three simulation cases discussed, alongside the resulting net plant efficiency and annual CO_2 emission.

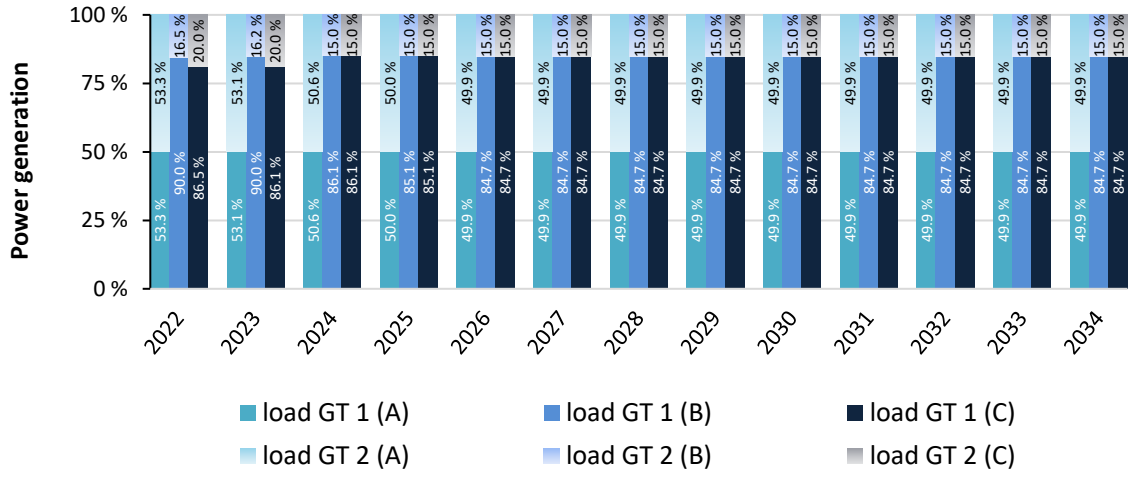

Figure 11. Annual share of power generation between the two offshore GTs. The length of the columns represents the fraction of the total power demand covered by the specific GT. The values embedded in the columns represent the GT load of the specific GT. The three cases represent the three operating strategies proposed, i.e. GTs + WHRU (A), (B) and (C).

It is worth pointing out that the discussed outcome of the optimal load allocation procedure is valid within the framework tested. With modified boundary conditions for the analysis (e.g. different power requirements), the situation may change, resulting in a different optimal share of power generation between the GTs. *Figure 12* helps to clarify the concept by showing the optimal load allocation for several different cases, covering the range of possible power outputs which can be supplied by the power generation unit of the offshore plant. A general trend can be outlined. For low power requirements, the optimal solution (C) basically matches the operating strategy (B), i.e. maximum possible load of one GT, while the other makes up the remaining power demand. This case is representative for most of the years characterizing the case study considered in this work. With increasing power requirements, the optimal solution (C) progressively shifts towards the other operating strategy (A), i.e. power demand equally split between the two GTs. One may argue that it should be good practice to implement such an analysis to define the best strategy for operating the GTs within the operating conditions set by a specific application.

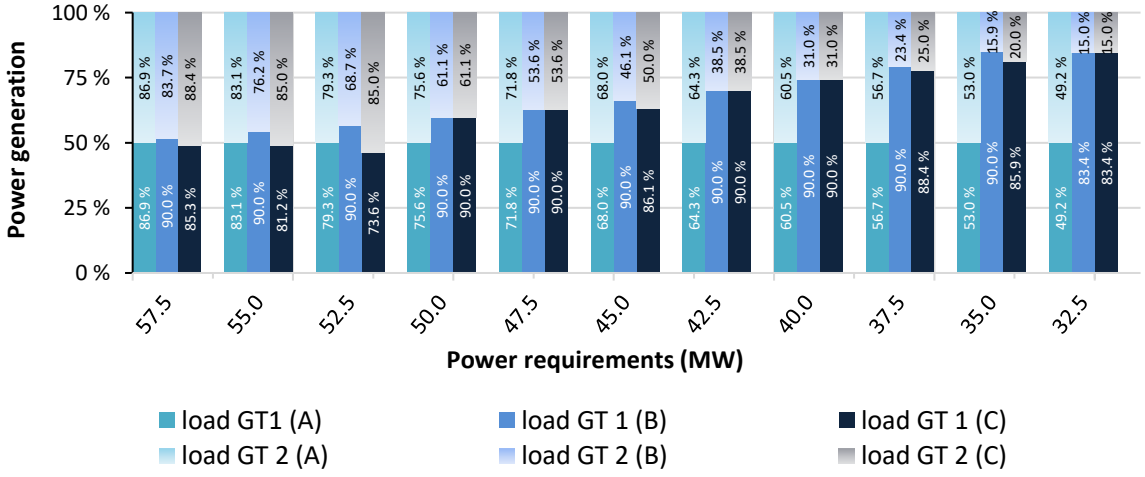

Figure 12. Share of power generation between the two offshore GTs for different power requirements. The length of the columns represents the share of the total plant load covered by the specific GT. The three cases represent the three operating strategies proposed, i.e. GTs + WHRU (A), (B) and (C).

6.2 Weight-to-heat rate optimization of the steam bottoming cycle design

The weight-to-heat rate optimization problem was set to define the best steam bottoming cycle design in terms of weight and net plant efficiency (through the heat rate). *Figure 13* shows the Pareto frontier returned by the algorithm. The algorithm stopped because a maximum number of iteration was reached. The high number of generations should ensure the reliability of the results. Such number is in line with the value selected in the literature for the design of offshore bottoming cycles [15]. Also the design of ORC using low grade heat source was based on similar assumptions [44]. However, since the function tolerance was not matched, an additional verification was carried out. The Pareto frontier was compared to those obtained when setting a lower maximum number of generations. It was verified that for a number of generations larger than 50, little improvements were noticed in the results. Thus, the results obtained were deemed as satisfactory for the type of analysis carried out in this paper. *Table 6* in the Appendix reports all the points of the Pareto frontier. *Table 4* shows the solutions returning minimum weight, minimum heat rate and the solution selected as the design point for further simulations. The design point was arbitrarily selected to be a compromise between weight and efficiency requirements.

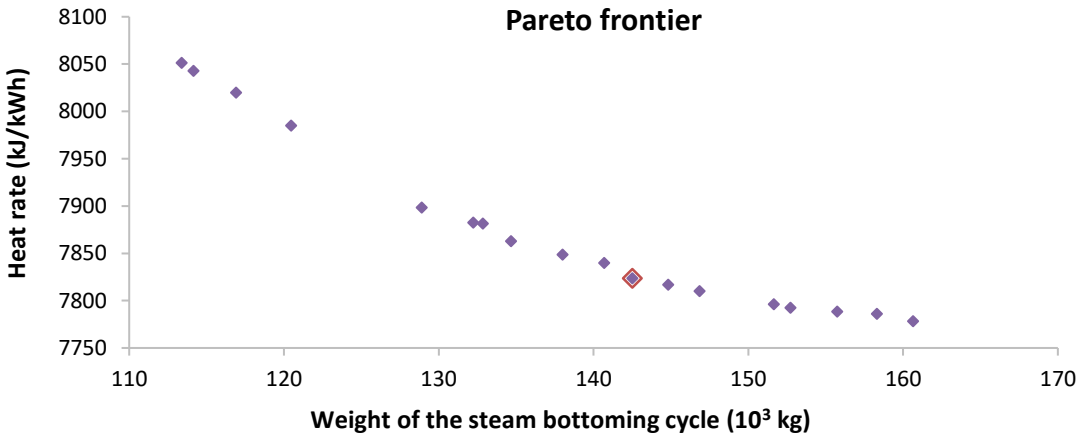

Figure 13. Pareto frontier of optimal solutions with regard to total plant heat rate and weight of the steam bottoming cycle. The solution used to define the design is also highlighted.

Table 4. Values of the decision variables and of the objective functions for three solutions. The solutions reported are that for minimum weight of the steam bottoming cycle, that for minimum total plant heat rate and that selected to be the design point.

	Minimum Weight	Minimum HR	Design point
Decision variables			
p_{steam} (bar)	15	27	20
T_{steam} (°C)	369	410	402
ΔT_{OTSG} (°C)	15	18	16
p_{cond} (bar)	0.12	0.03	0.04
ΔT_{cw} (°C)	10	10	10
Objective functions			
Weight (10^3 kg)	113	161	143
HR (kJ/kWh)	8051	7778	7823
$\eta_{net,plant}$	44.7 %	46.3 %	46.0 %

6.3 Lifetime performance of the different concepts

When considering different concepts for providing power and heat to the offshore plants, taking into account the entire lifetime allows a more complete overview. The same power and heat generation unit needs to be able to work efficiently in the several operational modes to which the plant will be subjected. Considering only fixed sets of operating conditions, corresponding to specific field's production periods, the outcome obtained could be misleading. The analysis presented in this work considers the off-design operation of the modeled systems, in accordance with averaged annual power and heat requirements. Since the ultimate objective was to minimize the total CO_2 emissions, this was the parameter to be monitored and analyzed. Before analyzing the results, some premises should be mentioned. Unlike the guidelines for a comprehensive comparative analysis, the obtained results, being based on a selected case study, cannot be generalized. Additionally, it can be expected that the tools used for the analysis, in particular the optimization algorithms, could be further refined leading to slightly improved results. However, the overall effect is expected to be limited, while other factors (partially addressed in the sensitivity analyses) are believed to contribute to a larger extent to the uncertainty of the analysis.

Figure 14 shows the cumulative CO_2 emissions for the period which was the subject of analysis (i.e. 2022 to 2034). The cumulative CO_2 emissions constitute the real measure of the effectiveness of the cases studied. All the cases simulated are reported.

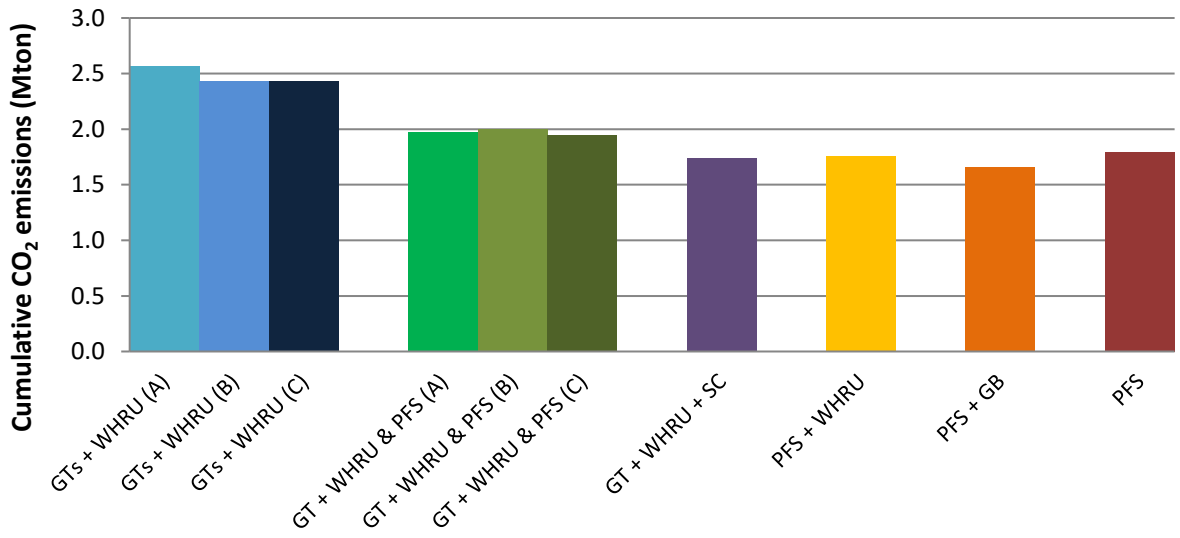

Figure 14. Cumulative CO_2 emissions for the different concepts studied for the period subject of analysis (i.e. 2022 to 2034).

In the first instance, it is possible to notice that a well-thought-out total plant load allocation between the GTs can already produce a sensible difference in the base concept relying on gas turbines and waste heat recovery unit. The optimized case GTs + WHRU (C) entails a reduction in the cumulative CO_2 emissions of 5.2%, in comparison to the common operating strategy simulated in case GTs + WHRU (A). Similarly, selecting the best share between local power generation and power from shore, depending on the specific operating conditions, is shown to be beneficial. In fact, the relative case GT + WHRU & PFS (C) outperforms the cases GT + WHRU & PFS (A) and GTs + WHRU & PFS (B), cutting cumulative CO_2 emissions down by 1.4% and 2.9% respectively. This shows how an effective energy management is able to produce improvements, even within the same system configuration. In this sense,

once a concept to supply power and heat is defined, the convenience of investigating the most suitable operating strategy, by taking into account the annual variations of operating conditions, is demonstrated.

Looking at the whole picture, remarkable reductions in cumulative CO_2 emissions are achieved when power is taken from the onshore grid, with the concept of relying on gas burners to provide process heat (i.e. PFS + GB) returning the best performance (- 35.5% CO_2 emissions compared to the base case GTs + WHRU (A)). Furthermore, the utilization of an offshore combined cycle (i.e. GT + WHRU + SC) showed the potential to be competitive with the concepts involving full electrification of the platform (- 32.2% CO_2 emissions). However, it is worth stressing that considerations regarding footprint and weight could question its feasibility and would need to be investigated more thoroughly. On the other hand, a local generation solution would not necessitate the significant investments associated with electrification of the plant. Further analyses should take into account all these factors, and an additional economic assessment would be advisable. Finally, it is worth offering a few words on the concept involving both local generation and power from shore (i.e. GT + WHRU & PFS). The obtained reduction in CO_2 emissions, although substantial (- 24.2% CO_2 emissions), is not on the same level as that of the other concepts. However, this hybrid solution is inherently more flexible, being able to shift between the two methods to supply power. It must be stressed that such a concept was made possible by the characteristics of the offshore plants studied, for which investments for both on-site power generation and electrification are already planned. For other cases, it is probable that the capital expenditures associated with this double investment would make the concept hardly feasible. Additional information can be grasped from *Figure 15*, which shows the annual CO_2 emissions with regard to the most interesting cases studied. For the sake of figure readability, not all the cases were reported. The rationale behind the choice of which cases to display lay in considering the best alternative among cases relying on the same system configuration but with different operating strategies. Thus, case GTs + WHRU (C) was selected over cases GTs + WHRU (A) and GTs + WHRU (B), and case GTs + WHRU & PFS (C) was selected over cases GTs + WHRU & PFS (A) and GTs + WHRU & PFS (B). Similarly, the concept named PFS + WHRU is not represented, being assessed as the least interesting among those involving platform electrification.

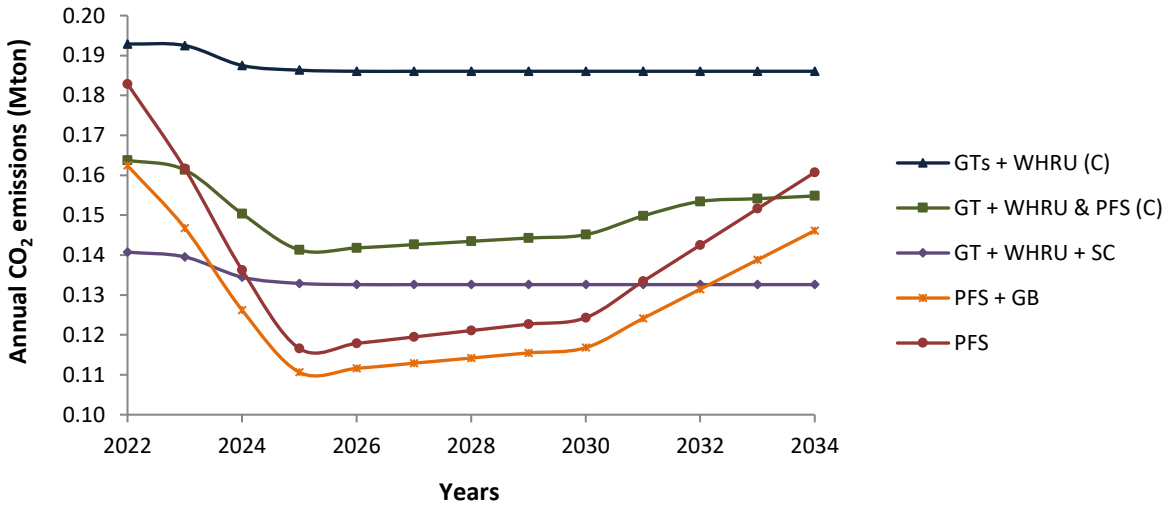

Figure 15. Annual CO_2 emissions of the most interesting cases studied, throughout the years considered in the analysis.

There is no single concept which outperforms the others in each year of the considered plant's lifetime. Evidently, concepts taking power from the onshore grid are particularly efficient when the relative CO_2

emission factor is low (i.e. 2025 to 2030). For higher CO_2 emission factors (i.e. first and last years of plant operation), the situation is overturned, with local power generation concepts becoming more efficient. One may also observe that the concepts involving full electrification of the offshore plant (i.e. PFS and PFS + GB) and the concept involving partial electrification (i.e. GTs + WHRU & PFS (C)) are those showing the higher variability of performances. On the contrary, concepts relying purely on on-site power generation (i.e. GT + WHRU (C) and GT + WHRU + SC) demonstrate steadier and more predictable performance, not being dependent on external factors like the short- and long-term variations of the power market.

The results discussed are heavily influenced by the modeling assumptions used. Differences in the power and heat demand profiles, in the equipment operating conditions and in the CO_2 emission factor could modify the outcome of the analysis. The more accurate is this set of information, the more reliable are the outputs. The next section investigates the influence of the parameter which is thought to have a strong impact on the results, namely the CO_2 emissions factor (χ_{CO2}). In addition, a sensitivity analysis of the plant's heat requirements is also presented.

6.4 Sensitivity analysis of carbon dioxide emission factor

For the cases relying to some extent on PFS, the CO_2 emissions were calculated by means of a χ_{CO2} trend suggested in the literature [17]. In order to evaluate how much the choice of χ_{CO2} affects the outcome of the analysis, a sensitivity analysis of such a parameter was carried out. Some significant values of χ_{CO2} were adopted. In particular, χ_{CO2} was set equal to the emission factor currently characterizing the Nordic (0.10 kg_{CO2}/kWh [29]), Norwegian (0.02 kg_{CO2}/kWh [30]) and European (0.43 kg_{CO2}/kWh [29]) power systems. When the European χ_{CO2} applies, the parameter taking into account the transmission losses on the power cables was increased to 15% considering the longer distance between the power generation and the consumer. *Figure 16* shows the cumulative CO_2 emissions obtained by applying the different values of χ_{CO2} to the same model. Similarly to *Figure 15*, only the most significant cases are reported.

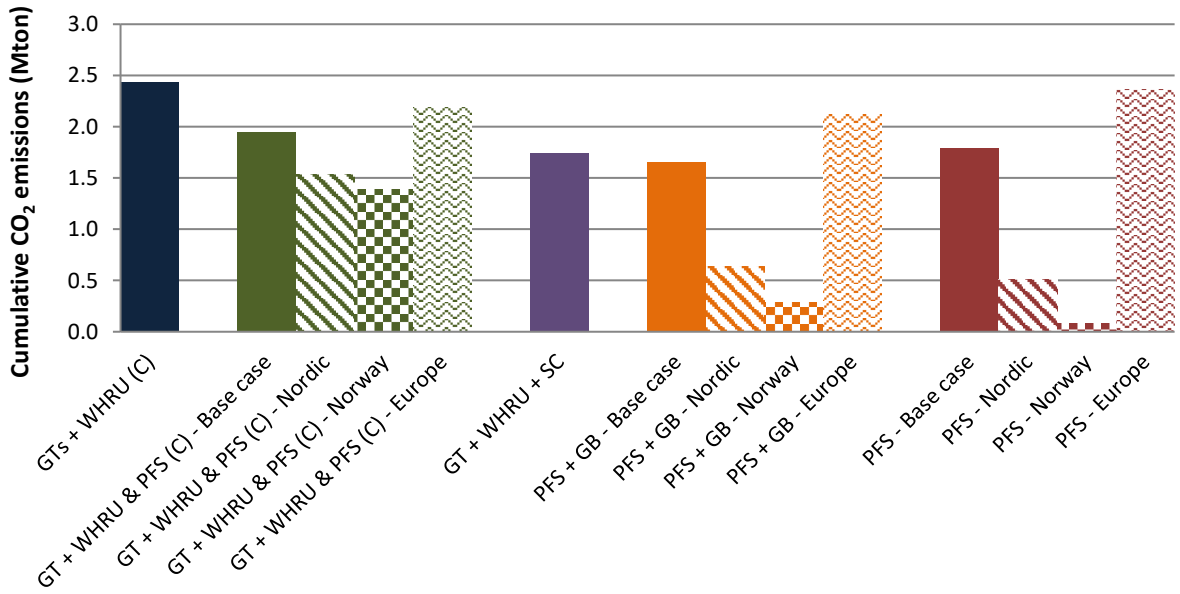

Figure 16. Cumulative CO_2 emissions for the most interesting cases studied for the period subject of analysis (i.e. 2022 to 2034), calculated with different CO_2 emission indexes associated to the power from shore. The emission indexes considered are: (i) that used as base case, that referring to (ii) the Nordic, (iii) the Norwegian and (iv) the European power systems.

As expected, the cases characterized by the largest variations are those relying more heavily on PFS. With the Nordic χ_{CO2}, the best case clearly becomes the one relying entirely on PFS. This situation is even more emphasized when the Norwegian χ_{CO2} is used. On the other hand, when applying the European χ_{CO2}, the convenience of using any PFS can be reasonably questioned. The real extent to which electrification could contribute to an overall reduction in CO_2 emissions has to be assessed through a comprehensive analysis of the power system. An understanding of how the marginal power to supply offshore would be generated and of the impact on the power and carbon market is fundamental in this sense.

6.5 Sensitivity analysis of plant heat requirements

The heat demand throughout the years considered in the analysis has been taken from the information retrieved in the available literature. Those values are estimations, thus subject to some degree of uncertainty. Since the amount of process heat to be supplied could be a key factor in the definition of the best plant concept, a sensitivity analysis has been carried out. The reference heat demand profile has been increased by 10%, 20% and 30%. *Figure 17* shows the cumulative CO_2 emissions obtained, when the concepts needed to comply with these new heat requirements.

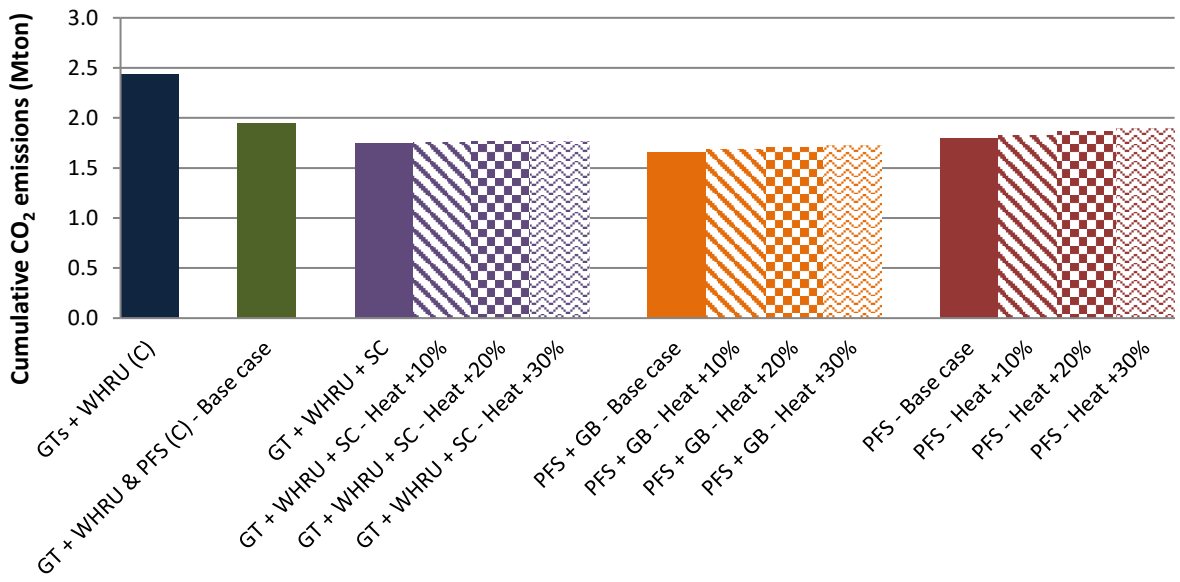

Figure 17. Cumulative CO_2 emissions for the most interesting cases studied for the period subject of analysis (i.e. 2022 to 2034), calculated with different process heat requirements. The heat requirements considered are: (i) that used as base case and the same one increased by (ii) 10%, (iii) 20% and (iv) 30%.

One may notice that the concepts relying on simple GT cycles to provide power and heat are not affected by different heat requirements. As long as there is enough thermal energy in the GT exhaust gas to supply heat to the processes, the plant performance remains unvaried. Among other concepts, those including PFS are the most influenced by augmented heat requirements. This can be ascribed to the method of supplying process heat. The cases with local power generation (e.g. GT + WHRU + SC) can exploit the exhaust gases of a GT though a WHRU. Such a method is thermodynamically more efficient than using a gas burner (e.g. PFS + GB) or an electric heater (e.g. PFS). Therefore, the higher the amount of heat to be supplied, the more penalized are those concepts not involving the operation of a GT. The

analysis seems to suggest that the convenience of electrifying the offshore facilities decreases with the increase in the plant's heat demand.

7. Conclusions

Different concepts for supplying power and heat to offshore installations were presented and investigated. A common framework was defined to carry out the comparative analysis, which involved the definition of the varying energy requirements associated with the oil and gas extraction, the detailed process modeling of the power generation units, and the optimization of the operating strategy. Off-design simulations were then carried out, taking into account the different operating conditions characterizing the life of the offshore plant. The performance of the different concepts was evaluated in terms of cumulative CO_2 emissions. The outlined approach was applied to a case study in the North Sea and proved to be effective in order to give a comprehensive assessment. Albeit the results obtained are case-specific and, thus, cannot be generalized, the same kind of analysis could be implemented to different installations.

As a first outcome, the importance of effective energy management, given a specific process framework and set of operating conditions, was stressed. An optimized total plant load allocation between the GTs of the plant was able to reduce the cumulative CO_2 emissions by 5.2% in comparison to the case representing the conservative strategy commonly used in offshore applications.

When comparing the different concepts studied, the full electrification of the plant was shown to entail the largest possible cut in CO_2 emissions. In particular, the best concept was demonstrated to be that of taking power from the onshore grid and providing heat through gas burners installed on the platforms, with a potential reduction in cumulative CO_2 emissions of up to 35.5%. Similarly, good performance was obtained by the concept involving a combined cycle for on-site power generation (CO_2 emission reduction: 32.2%). The specificity of the analyzed offshore platforms allowed an additional hybrid solution to be evaluated. This involved the possibility of exploiting both on-site power generation and power from shore. The obtained CO_2 emissions reduction was not as good as in the case of the other concepts proposed (24.2%), but inherent higher plant flexibility is a potentially interesting advantage.

A series of model assumptions was made for the analysis, which may have a strong influence on the results. In that regard, a sensitivity analysis was carried out on the considered CO_2 emission factor, the parameter which defines the CO_2 emissions per unit of power taken from the onshore grid. The analysis demonstrated how different values of this parameter can substantially modify the outcomes. A detailed evaluation of the power system of interest is therefore suggested in order to understand the real benefits connected to the electrification of offshore facilities. A further sensitivity analysis of the offshore plant's heat demand showed that the energy advantages associated with the electrification of the facilities tend to diminish with the increase in heat requirements.

Acknowledgments

This publication has been produced with support from Lundin Norway AS within the research project "Electrification and efficient energy supply of offshore oil platforms".

References

[1] Statistisk Sentralbyrå. Utslipp av klimagasser, 2015 2016. http://www.ssb.no/natur-og-miljo/statistikker/klimagassn/.

[2] Ministry of Petroleum and Energy, Norwegian Petroleum Directorate. Norsk Petroleum 2017. http://www.norskpetroleum.no/.

[3] Nguyen T-V, Pierobon L, Elmegaard B, Haglind F, Breuhaus P, Voldsund M. Exergetic assessment of energy systems on North Sea oil and gas platforms. Energy 2013;62:23–6.

[4] Nguyen T Van, Jacyno T, Breuhaus P, Voldsund M, Elmegaard B. Thermodynamic analysis of an upstream petroleum plant operated on a mature field. Energy 2014;68:454–69.

[5] Voldsund M, Ertesvåg IS, He W, Kjelstrup S. Exergy analysis of the oil and gas processing on a north sea oil platform a real production day. Energy 2013;55:716–27.

[6] Voldsund M, Nguyen T-V, Elmegaard B, Ertesvåg IS, Røsjorde A, Jøssang K, et al. Exergy destruction and losses on four North Sea offshore platforms: A comparative study of the oil and gas processing plants. Energy 2014;74:45–58.

[7] De Oliveira S, Van Hombeeck M. Exergy analysis of petroleum separation processes in offshore platforms. Energy Convers Manag 1997;38:1577–84.

[8] Nord LO, Bolland O. Steam bottoming cycles offshore - Challenges and possibilities. J Power Technol 2012;92:201--207.

[9] Kloster P. Reduction of Emissions to Air Through Energy Optimisation on Offshore Installations. Proc. SPE Int. Conf. Heal. safety, Environ. oil gas Explor. Prod., Stavanger (Norway): 2000, p. 1–7.

[10] Nord LO, Bolland O. Design and off-design simulations of combined cycles for offshore oil and gas installations. Appl Therm Eng 2013;54:85–91.

[11] Riboldi L, Nord LO. Lifetime Assessment of Combined Cycles for Cogeneration of Power and Heat in Offshore Oil and Gas Installations. Energies 2017;10:744.

[12] Pierobon L, Nguyen T Van, Larsen U, Haglind F, Elmegaard B. Multi-objective optimization of organic Rankine cycles for waste heat recovery: Application in an offshore platform. Energy 2013;58:538–49.

[13] Barrera JE, Bazzo E, Kami E. Exergy analysis and energy improvement of a Brazilian floating oil platform using Organic Rankine Cycles. Energy 2015;88:67–79.

[14] Bhargava RK, Bianchi M, Branchini L, De Pascale A, Orlandini V. Organic Rankine cycle system for effective energy recovery in offshore applications: a parametric investigation with different power rating gas turbines. Proc. ASME Turbo Expo 2015, Montréal: 2015.

[15] Pierobon L, Benato A, Scolari E, Haglind F, Stoppato A. Waste heat recovery technologies for offshore platforms. Appl Energy 2014;136:228–41.

[16] Walnum HT, Nekså P, Nord LO, Andresen T. Modelling and simulation of CO2 (carbon dioxide) bottoming cycles for offshore oil and gas installations at design and off-design conditions. Energy 2013;59:513–20.

[17] Econ Pöyry. CO2-emissions effect of electrification. 2011.

[18] He W, Uhlen K, Hadiya M, Chen Z, Shi G, Rio E. Case Study of Integrating an Offshore Wind Farm with Offshore Oil and Gas Platforms and with an Onshore Electrical Grid. Renew Energy 2014;2013:5–9.

[19] Kolstad ML, Årdal AR, Sharifabadi K, Undeland TM. Integrating Offshore Wind Power and Multiple Oil and Gas Platforms to the Onshore Power Grid Using VSC-HVDC Technology. Mar Technol Soc J 2014;48:31–44.

[20] Nguyen T-V, Tock L, Breuhaus P, Maréchal F, Elmegaard B. CO2-mitigation options for the offshore oil and gas sector. Appl Energy 2016;161:673–94.

[21] Korpås M, Warland L, He W, Tande JOG. A case-study on offshore wind power supply to oil and gas rigs. Energy Procedia, vol. 24, 2012, p. 18–26.

[22] Marzband M, Sumper A, Domínguez-García JL, Gumara-Ferret R. Experimental validation of a real time energy management system for microgrids in islanded mode using a local day-ahead electricity market and MINLP. Energy Convers Manag 2013;76:314–22.

[23] Nguyen T Van, Fülop TG, Breuhaus P, Elmegaard B. Life performance of oil and gas

platforms: Site integration and thermodynamic evaluation. Energy 2014;73:282–301.
[24] Margarone M, Magi S, Gorla G, Biffi S, Siboni P, Valenti G, et al. Revamping, Energy Efficiency, and Exergy Analysis of an Existing Upstream Gas Treatment Facility. J Energy Resour Technol 2011;133:12001.
[25] Mazzetti JM, Nekså P, Walnum HT, Hemmingsen AKT. Energy-Efficient Technologies for Reduction of Offshore CO2 Emmissions. Offshore Technol. Conf., Houston: 2013.
[26] Statoil. Power solutions for Johan Sverdrup field in phase 1 and for full field. 2014.
[27] Lundin, Wintershall, RWE. Plan for utbygging, anlegg og drift av Luno - Del 2: Konsekvensutredning. 2011.
[28] Det norske oljeselskap ASA. Plan for utbygging og drift av Ivar Aasen - Del 2: Konsekvensutredning. 2012.
[29] Norden, IEA. Nordic Energy Technology Perspectives - Pathways to a Carbon Neutral Energy Future. 2013.
[30] IEA. CO2 emissions from fuel combustion - Highlights. Oecd/Iea 2015;S/V:1–139.
[31] Thermoflow Inc. Thermoflex Version 26.0 2016.
[32] ESCOA Corp. ESCOA Fintube Manual. Tulsa, OK, USA: 1979.
[33] Nord LO, Martelli E, Bolland O. Weight and power optimization of steam bottoming cycle for offshore oil and gas installations. Energy 2014;76:891–8.
[34] Spencer RC, Cotton KC, Cannon CN. A method for predicting the performance of steam turbine generators 16,500 kW and larger. J Eng Power 1963;85:249–98.
[35] Kehlhofer R. Combined-cycle Gas & Steam Turbine Power Plants. 1999.
[36] Baldi F, Ahlgren F, Melino F, Gabrielii C, Andersson K. Optimal load allocation of complex ship power plants. Energy Convers Manag 2016;124:344–56.
[37] Rios LM, Sahinidis N V. Derivative-free optimization: A review of algorithms and comparison of software implementations. J. Glob. Optim., vol. 56, 2013, p. 1247–93.
[38] Martelli E, Amaldi E. PGS-COM: A hybrid method for constrained non-smooth black-box optimization problems. Brief review, novel algorithm and comparative evaluation. Comput Chem Eng 2014;63:108–39. doi:10.1016/j.compchemeng.2013.12.014.
[39] Holland JH. Adaptation in Natural and Artificial Systems. vol. Ann Arbor. 1975. doi:10.1137/1018105.
[40] Ahmadi P, Dincer I, Rosen MA. Exergy, exergoeconomic and environmental analyses and evolutionary algorithm based multi-objective optimization of combined cycle power plants. Energy 2011;36:5886–98.
[41] MathWorks. Global optimization toolbox. 2016.
[42] Toffolo A, Lazzaretto A. Evolutionary algorithms for multi-objective energetic and economic optimization in thermal system design. Energy 2002;27:549–67.
[43] Abraham A, Jain L, Goldberg R. Evolutionary Multi-objective Optimization: Theoretical Advances and Applications. Springer London; 2005. doi:10.1007/1-84628-137-7.
[44] Wang J, Yan Z, Wang M, Ma S, Dai Y. Thermodynamic analysis and optimization of an (organic Rankine cycle) ORC using low grade heat source. Energy 2013;49:356–65.

Appendix

Table 5. Main performance of the three cases studied assuming on-site power and heat generation through gas turbines and a waste heat recovery unit (i.e. GT + WHRU (A), (B) and (C)). The parameters reported are GT loads, net plant efficiency and CO_2 emissions for each year analysed of the offshore plants life.

	GTs + WHRU (A)				GTs + WHRU (B)				GTs + WHRU (C)			
Years	**load GT1**	**load GT2**	**$\eta_{net,plant}$**	**Mton CO_2**	**load GT1**	**load GT2**	**$\eta_{net,plant}$**	**Mton CO2**	**load GT1**	**load GT2**	**$\eta_{net,plant}$**	**Mton CO_2**
2022	53.3 %	53.3 %	30.3 %	0.209	90.0 %	16.5 %	32.7 %	0.194	86.5 %	20.0 %	32.8 %	0.193
2023	53.1 %	53.1 %	30.3 %	0.208	90.0 %	16.2 %	32.6 %	0.193	86.1 %	20.0 %	32.8 %	0.193
2024	50.6 %	50.6 %	30.4 %	0.198	86.1 %	15.0 %	32.0 %	0.187	86.1 %	15.0 %	32.0 %	0.187
2025	50.0 %	50.0 %	30.4 %	0.196	85.1 %	15.0 %	31.9 %	0.186	85.1 %	15.0 %	31.9 %	0.186
2026	49.9 %	49.9 %	30.3 %	0.195	84.7 %	15.0 %	31.8 %	0.186	84.7 %	15.0 %	31.8 %	0.186
2027	49.9 %	49.9 %	30.3 %	0.195	84.7 %	15.0 %	31.8 %	0.186	84.7 %	15.0 %	31.8 %	0.186
2028	49.9 %	49.9 %	30.3 %	0.195	84.7 %	15.0 %	31.8 %	0.186	84.7 %	15.0 %	31.8 %	0.186
2029	49.9 %	49.9 %	30.3 %	0.195	84.7 %	15.0 %	31.8 %	0.186	84.7 %	15.0 %	31.8 %	0.186
2030	49.9 %	49.9 %	30.3 %	0.195	84.7 %	15.0 %	31.8 %	0.186	84.7 %	15.0 %	31.8 %	0.186
2031	49.9 %	49.9 %	30.3 %	0.195	84.7 %	15.0 %	31.8 %	0.186	84.7 %	15.0 %	31.8 %	0.186
2032	49.9 %	49.9 %	30.3 %	0.195	84.7 %	15.0 %	31.8 %	0.186	84.7 %	15.0 %	31.8 %	0.186
2033	49.9 %	49.9 %	30.3 %	0.195	84.7 %	15.0 %	31.8 %	0.186	84.7 %	15.0 %	31.8 %	0.186
2034	49.9 %	49.9 %	30.3 %	0.195	84.7 %	15.0 %	31.8 %	0.186	84.7 %	15.0 %	31.8 %	0.186

Table 6. Points of the Pareto frontier obtained in the multi-objective design optimization of the steam bottoming cycle. The points represent Pareto-optimum solutions with respect to minimum heat rate and weight.

Pareto point	**Decision variables**					**Objective functions**		
	p_{steam} (bar)	**T_{steam} (°C)**	**ΔT_{OTSG} (°C)**	**p_{cond} (bar)**	**ΔT_{cw} (°C)**	**Weight (10^3 kg)**	**HR (kJ/kWh)**	**$\eta_{net.plant}$**
1	15.0	368.7	14.7	0.118	9.7	113.4	8051	44.7 %
2	15.7	370.3	14.5	0.116	9.7	114.1	8043	44.8 %
3	17.9	370.2	15.2	0.108	9.9	116.9	8020	44.9 %
4	19.2	380.2	16.5	0.097	9.9	120.5	7985	45.1 %
5	16.8	382.9	14.8	0.052	9.8	128.9	7898	45.6 %
6	19.7	389.6	15.7	0.053	9.8	132.8	7881	45.7 %
7	19.1	403.7	17.7	0.056	9.8	132.2	7882	45.7 %
8	17.5	393.6	15.2	0.044	9.8	134.7	7863	45.8 %
9	20.1	382.3	16.4	0.041	9.8	138.0	7849	45.9 %
10	22.4	392.5	16.2	0.043	9.8	140.7	7840	45.9 %
11	19.9	401.6	16.3	0.037	9.7	142.5	7823	46.0 %
12	21.1	401.7	16.7	0.036	9.8	144.8	7817	46.1 %
13	22.3	398.9	17.0	0.035	9.9	146.8	7810	46.1 %
14	21.5	405.4	17.1	0.031	9.8	151.6	7796	46.2 %
15	22.4	405.4	17.5	0.032	9.9	152.7	7792	46.2 %
16	24.8	404.4	17.4	0.031	9.9	155.7	7788	46.2 %
17	27.0	402.9	16.9	0.032	10.0	158.3	7786	46.2 %
18	27.0	409.9	17.7	0.031	10.0	160.6	7778	46.3 %